Mathematics in Applied Sciences and Engineering
Volume **6**, Number **2**, June **2025**, pp.**157-173**

https://ojs.lib.uwo.ca/mase
https://doi.org/10.5206/mase/22269

DYNAMICAL ANALYSIS OF A MONKEYPOX SPREAD MODEL WITH HUMAN TO HUMAN SATURATED INCIDENCE RATE AND ENVIRONMENTAL TRANSMISSION

BRAZIL VARGAS JUNIOR POSSUMAH, WURYANSARI MUHARINI KUSUMAWINAHYU, AND TRISILOWATI

Abstract. In this paper, we study the behavior of monkeypox spread by constructing a compartmental model describing virus transmission between humans, animals, and the environment. The model incorporates vaccination on susceptible humans, quarantine on exposed humans, and hospitalization on infected humans. A saturated incidence rate is applied to obtain a more realistic model. The model's basic reproduction number (R_0) is obtained by applying the next-generation matrix method. The analysis shows that the local stability of the equilibrium points depends on the value of R_0, and it is also shown that the model undergoes forward bifurcation. Furthermore, sensitivity analysis and numerical simulations were conducted to illustrate the analytical results.

1. Introduction

Monkeypox, caused by the monkeypox virus, is primarily zoonotic. Transmission to humans commonly originates from wild animal reservoirs such as rodents and primates. However, human-to-human transmission is also prevalent [9]. Human transmission occurs via direct contact with bodily fluids, contaminated surfaces, or infectious lesions of infected individuals [2, 9]. Symptoms include fever, headache, muscle aches, back pain, fatigue, skin lesions, and swollen lymph nodes [2]. The incubation period ranges from 5-21 days, usually around 6-16 days [17]. As of August 2024, there have been 103,446 confirmed cases and 225 deaths globally [13].

Mathematical models play a crucial role in analyzing the spread of infectious diseases and their impact on populations. Bhunu and Mushayabasa [4] proposed a model to describe the transmission dynamics of monkeypox in humans and animals. Usman and Adamu [20] added an exposed compartment and assumed permanent immunity from vaccination, while Peter et al. [17] introduced a quarantine compartment for exposed humans. Madubueze et al. [11] combined these models, assuming vaccines do not provide permanent immunity and include environmental transmission. Alshehri and Ullah [1] conducted a similar study, considering the spread of the virus through human interaction with a contaminated environment and the quarantine of exposed humans. Majee et al. [12] added a compartment for the hospitalization of infected humans and vaccination. Okongo et al. [16] categorized infected humans into symptomatic and asymptomatic cases, with hospitalization for symptomatic cases. These models apply bilinear and standard incidence rates for human-to-human transmission. However, as the infected population grows, these rates become less realistic, as they fail to take into account the behavioral responses of susceptible individuals—such as self-isolation, improved hygiene, and other preventive actions—that can reduce transmission of the disease [22].

Received by the editors 18 December 2024; accepted 14 April 2025; published online 2 June 2025.
2020 *Mathematics Subject Classification.* 34A34, 37N25, 92B05.
Key words and phrases. Monkeypox model, saturated incidence rate, contaminated environment, local stability, forward bifurcation.

The saturated incidence rate, introduced by Capasso and Serio [5], considers behavioral changes in susceptibles as the infected population increases. Few existing monkeypox models incorporate saturated incidence rates, with many focusing separately on specific interventions such as vaccination, quarantine, or treatment. In contrast, this study presents a more comprehensive framework that not only integrates environmental transmission and saturated incidence rate for human-to-human transmission but also considers all these interventions within a single model. By incorporating vaccination for susceptible individuals, quarantine for exposed cases, and hospitalization for infected individuals, our model offers a more realistic representation of disease dynamics and the effectiveness of intervention strategies.

This study employs dynamical analysis to establish the positivity and boundedness of the solutions, determine the equilibrium point, and analyze its local stability. The possibility of forward bifurcation is also investigated, as well as the parameter sensitivity analysis. Finally, numerical simulations are performed to illustrate the analytical results.

2. Model formulation

This model considers three populations: the human population, the animal population, and the virus population within a contaminated environment. The human population is divided into seven compartments: susceptible humans (S_h), vaccinated humans (V_h), exposed humans (E_h), quarantined humans (Q_h), infected humans (I_h), hospitalized humans (H_h), and recovered humans (R_h). The animal population is categorized into two compartments: susceptible animals (S_r) and infected animals (I_r). There is a single compartment for the virus population in the environment, C. The sizes of all three populations—humans, animals, and the virus in the environment—are considered in terms of population density. The model is constructed under the following assumptions:

(1) Vaccines given to susceptible humans do not provide permanent immunity [11, 8].
(2) Saturated incidence rate is used for human-to-human virus transmission.
(3) Virus transmission for human-to-animal, human-to-environment, and animal-to-animal follows a bilinear incidence rate.
(4) Quarantined humans may become infected or recover naturally [17].
(5) Infected humans must be hospitalized to recover fully [16].
(6) Viruses in contaminated environment increase due to the shedding of viruses by infected humans and animals [11].

Based on these assumptions, the spread of monkeypox is illustrated as a compartmental diagram in Fig. 1 and is modeled as a system of nonlinear differential equations (2.1), with the parameters described in Table 1.

$$\begin{cases} \dot{S_h} = \Lambda_h + \phi V_h - (\beta + m_1) S_h \\ \dot{V_h} = \epsilon S_h - m_2 V_h \\ \dot{E_h} = \beta S_h - m_3 E_h \\ \dot{Q_h} = \sigma_1 E_h - m_4 Q_h \\ \dot{I_h} = \sigma_2 E_h + \theta_2 Q_h - m_5 I_h \\ \dot{H_h} = \gamma I_h - m_6 H_h \\ \dot{R_h} = \theta_1 Q_h + \nu H_h - \mu_h R_h \\ \dot{S_r} = \Lambda_r - (\beta_4 I_r + \mu_r) S_r \\ \dot{I_r} = \beta_4 S_r I_r - m_7 I_r \\ \dot{C} = \rho_r I_r + \rho_h I_h - \mu_C C, \end{cases} \tag{2.1}$$

where $\beta = \frac{\beta_1 I_h}{1+\alpha_1 I_h} + \beta_2 I_r + \beta_3 C$, $m_1 = \epsilon + \mu_h$, $m_2 = \phi + \mu_h$, $m_3 = \sigma_1 + \sigma_2 + \mu_h$, $m_4 = \theta_1 + \theta_2 + \mu_h$, $m_5 = \gamma + \mu_h + \delta_h$, $m_6 = \nu + \mu_h + \delta_h$, and $m_7 = \mu_r + \delta_r$. These terms are introduced to simplify the expressions in model (2.1). The initial conditions of model (2.1) are $S_h(0) > 0, V_h(0) > 0, E_h(0) \geq 0, Q_h(0) \geq 0, I_h(0) \geq 0, H_h(0) \geq 0, R_h(0) \geq 0, S_r(0) > 0, I_r(0) \geq 0$, and $C(0) \geq 0$.

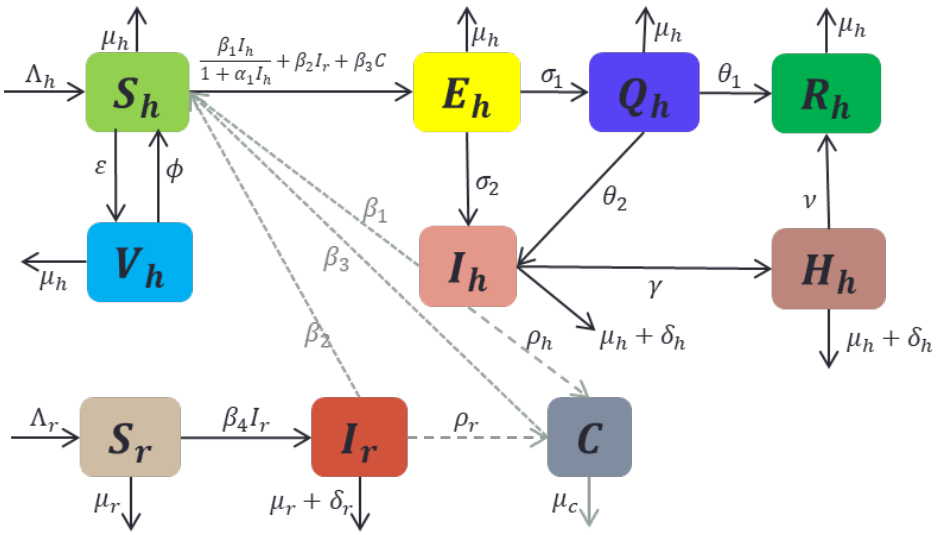

FIGURE 1. Compartmental diagram of the proposed monkeypox model

TABLE 1. Model parameters descriptions and estimations

Parameter	Description	Value	Source
Λ_h	Recruitment rate of susceptible humans	800	[11]
Λ_r	Recruitment rate of susceptible animals	0.2	[11]
μ_h	Natural mortality rate of human population	0.2	[11]
μ_r	Natural mortality rate of animal population	0.3	[11]
δ_h	Monkeypox-induced mortality rate of human population	0.02	[16]
δ_r	Monkeypox-induced mortality rate of animal population	0.4	[16]
β_1	Effective contact rate between susceptible and infected humans	0.000063	[11]
β_2	Effective contact rate between susceptible humans and infected animals	0.0027	[16]
β_3	Effective contact rate between susceptible humans and virus in contaminated environments	3.08×10^{-7}	[1]
β_4	Effective contact rate between susceptible and infected animals	0.027	[16]
α_1	Inhibition rate in human-to human transmission	$(0, 1]$	Assumed*
ϵ	Vaccination rate of susceptible humans	$[0.1, 1]$	[11]
ϕ	Immunity waning rate of vaccinated humans	0.095	[11]
σ_1	Quarantine rate of exposed humans	0.481	[16]
σ_2	Infection rate of exposed humans	0.2	[11]
θ_1	Recovery rate of quarantined humans	0.52	[12]
θ_2	Infection rate of quarantined humans	0.52	[11]
γ	Hospitalization rate of infected humans	0.03	[16]
ν	Recovery rate of hospitalized humans	0.036	[16]
ρ_h	Virus shedding rate by infected humans	0.04	[11]
ρ_r	Virus shedding rate by infected animals	0.02	[11]
μ_C	Natural disappearance rate of viruses in the environment	0.003	[11]

*Due to the limited literature on monkeypox models incorporating a saturated human-to-human incidence rate, the assumption for the value of α_1 is based on [18, 3], which explore epidemic models in general by applying a saturated incidence rate.

3. Positivity and boundedness of the solutions

Theorem 3.1. *For non-negative initial conditions, the solution of model (2.1) is non-negative, for all $t > 0$, and ultimately bounded on the invariant region*

$$\Gamma = \left\{ (S_h, V_h, E_h, Q_h, I_h, H_h, R_h, S_r, I_r, C) \in \mathbb{R}^{10}_+ : N_h \leq \frac{\Lambda_h}{\mu_h}, N_r \leq \frac{\Lambda_r}{\mu_r}, C \leq \frac{1}{\mu_C}\left(\frac{\rho_h \Lambda_h}{\mu_h} + \frac{\rho_r \Lambda_r}{\mu_r}\right) \right\},$$

where $N_h = S_h + V_h + E_h + Q_h + I_h + H_h + R_h$ and $N_r = S_r + I_r$.

Proof. Suppose $S_h(t) < 0$ and $V_h(t) < 0$ for some $t > 0$. Then there exist $t_1 > 0$ and $t_2 > 0$ such that: $S_h(t) > 0$ for $t < t_1$ and $S_h(t) < 0$ for $t > t_1$; $V_h(t) > 0$ for $t < t_2$ and $V_h(t) < 0$ for $t > t_2$; and $S_h(t_1) = V_h(t_2) = 0$. If $t_1 \leq t_2$, then $V_h(t_1) \geq 0$, and

$$\dot{S_h}|_{t=t_1} = \Lambda_h + \phi V_h(t_1) > 0. \tag{3.1}$$

Thus, $S_h(t) > 0$ for $t \in (t_1, t_1 + \varepsilon_1)$ for some $\varepsilon_1 > 0$. This leads to a contradiction. Hence, $S_h(t) > 0$ for all $t > 0$. Consequently,

$$\dot{V_h}|_{t=t_2} = \epsilon S_h(t_2) > 0. \tag{3.2}$$

This implies $V_h(t) > 0$ for $t \in (t_2, t_2 + \varepsilon_1)$ for some $\varepsilon_1 > 0$. This is a contradiction, so $V_h(t) > 0$ for all $t > 0$.

For $t_1 > t_2$, since $S_h(t_2) > 0$, (3.2) holds, leading to $V_h(t) > 0$ in $(t_2, t_2 + \varepsilon_1)$, again a contradiction. Thus, $V_h(t) > 0$ for all $t > 0$, and subsequently, (3.1) follows, ensuring $S_h(t) > 0$ in $(t_1, t_1 + \varepsilon_1)$, which also leads to contradiction. Therefore, $S_h(t) > 0$ for all $t > 0$. Based on both cases, $S_h(t) > 0$ and $V_h(t) > 0$ for all $t > 0$. Applying the similar way, the positivity for the variables E_h, Q_h, I_h, H_h, R_h, S_r, I_r, and C can be obtained.

The boundedness of the solutions is proven by noting that

$$\dot{N_h} \leq \Lambda_h - \mu_h N_h,$$
$$\dot{N_r} \leq \Lambda_r - \mu_r N_r.$$

Based on the comparison theory [10],

$$N_h(t) \leq N_h(0)e^{-\mu_h t} + \frac{\Lambda_h}{\mu_h}\left(1 - e^{-\mu_h t}\right),$$
$$N_r(t) \leq N_r(0)e^{-\mu_r t} + \frac{\Lambda_r}{\mu_r}\left(1 - e^{-\mu_r t}\right).$$

Observe that $\lim_{t\to\infty} N_h(t) \leq \Lambda_h/\mu_h$ and $\lim_{t\to\infty} N_r(t) \leq \Lambda_r/\mu_r$. Based on these results, $I_h \leq \Lambda_h/\mu_h$ and $I_r \leq \Lambda_r/\mu_r$, thus

$$\begin{aligned}\dot{C} &= \rho_h I_h + \rho_r I_r - \mu_C C \\ &\leq \rho_h \left(\frac{\Lambda_h}{\mu_h}\right) + \rho_r \left(\frac{\Lambda_r}{\mu_r}\right) - \mu_C C.\end{aligned}$$

Hence,

$$C(t) \leq C(0)e^{-\mu_C t} + \frac{1}{\mu_C}\left(\frac{\rho_h \Lambda_h}{\mu_h} + \frac{\rho_r \Lambda_r}{\mu_r}\right)\left(1 - e^{-\mu_C t}\right),$$

and

$$\lim_{t\to\infty} C(t) \leq \frac{1}{\mu_C}\left(\frac{\rho_h \Lambda_h}{\mu_h} + \frac{\rho_r \Lambda_r}{\mu_r}\right).$$

□

4. Equilibrium points and basic reproduction number

Model (2.1) has three equilibrium points. The first equilibrium point is the monkeypox-free equilibrium point, which is when $E_h = Q_h = I_h = H_h = R_h = I_r = C = 0$. This equilibrium point can be expressed as

$$E_0 = (S_h^0, V_h^0, 0, 0, 0, 0, 0, S_r^0, 0, 0),$$

where

$$S_h^0 = \frac{\Lambda_h m_2}{m_1 m_2 - \epsilon\phi}, \quad V_h^0 = \frac{\epsilon S_h^0}{m_2}, \quad S_r^0 = \frac{\Lambda_r}{\mu_r}$$

and $m_1 m_2 - \epsilon\phi = \mu_h(\epsilon + \phi) + \mu_h^2 > 0$. E_0 always exists and represents the condition where there is no disease in the populations.

The basic reproduction number (R_0) is the average number of secondary infections generated by a single infected individual in a fully susceptible population throughout their infectious period [15]. The R_0 of model (2.1) is obtained using the next-generation matrix method [14]. Let $\vec{Z} = (E_h, Q_h, I_h, H_h, I_r, C)$ be a vector containing infected individual compartments. Based on model (2.1), we get

$$\frac{d\vec{Z}}{dt} = \mathcal{F}_i - \mathcal{V}_i,$$

where

$$\mathcal{F}_i = \begin{pmatrix} \beta S_h \\ 0 \\ 0 \\ 0 \\ \beta_4 S_r I_r \\ 0 \end{pmatrix} \quad \text{and} \quad \mathcal{V}_i = \begin{pmatrix} m_3 E_h \\ -\sigma_1 E_h + m_4 Q_h \\ -\sigma_2 E_h - \theta_2 Q_h + m_5 I_h \\ -\gamma I_h + m_6 H_h \\ m_7 I_r \\ -\rho_r I_r - \rho_h I_h + \mu_C C \end{pmatrix}.$$

The Jacobian matrices of $\mathcal{F}_i$ and $\mathcal{V}_i$ around E_0, F and V, are as follows.

$$F = \begin{pmatrix} 0 & 0 & \beta_1 S_h^0 & 0 & \beta_2 S_h^0 & \beta_3 S_h^0 \\ 0 & 0 & 0 & 0 & 0 & 0 \\ 0 & 0 & 0 & 0 & 0 & 0 \\ 0 & 0 & 0 & 0 & 0 & 0 \\ 0 & 0 & 0 & 0 & \beta_4 S_r^0 & 0 \\ 0 & 0 & 0 & 0 & 0 & 0 \end{pmatrix} \quad \text{and} \quad V = \begin{pmatrix} m_3 & 0 & 0 & 0 & 0 & 0 \\ -\sigma_1 & m_4 & 0 & 0 & 0 & 0 \\ -\sigma_2 & -\theta_2 & m_5 & 0 & 0 & 0 \\ 0 & 0 & -\gamma & m_6 & 0 & 0 \\ 0 & 0 & 0 & 0 & m_7 & 0 \\ 0 & 0 & -\rho_h & 0 & -\rho_r & \mu_C \end{pmatrix}.$$

Hence, we obtained the next-generation matrix

$$K = FV^{-1} = \begin{pmatrix} R_{0H} & \frac{S_h^0(\beta_1\mu_C + \beta_3\rho_h)}{m_4 m_5 \mu_C} & \frac{S_h^0(\beta_1\mu_C + \beta_3\rho_h)}{m_5\mu_C} & 0 & \frac{S_h^0(\beta_2\mu_C + \beta_3\rho_r)}{m_7\mu_C} & \frac{\beta_3 S_h^0}{\mu_C} \\ 0 & 0 & 0 & 0 & 0 & 0 \\ 0 & 0 & 0 & 0 & 0 & 0 \\ 0 & 0 & 0 & 0 & 0 & 0 \\ 0 & 0 & 0 & 0 & R_{0R} & 0 \\ 0 & 0 & 0 & 0 & 0 & 0 \end{pmatrix},$$

where

$$R_{0H} = \frac{\beta_1 S_h^0(m_4\sigma_2 + \sigma_1\theta_2)}{m_3 m_4 m_5} + \frac{\beta_3 S_h^0 \rho_h (m_4\sigma_2 + \sigma_1\theta_2)}{m_3 m_4 m_5 \mu_C}, \tag{4.1}$$

$$R_{0R} = \frac{\beta_4 S_r^0}{m_7}.$$

Since R_0 defined as the maximum of the modulus of the eigenvalues (spectral radius) of K, we get

$$R_0 = \max(R_{0H}, R_{0R}).$$

R_{0H} represents the basic reproduction number for virus transmission involving humans and the environment, while R_{0R} corresponds to virus transmission among animals. Furthermore, in (4.1), the first term of R_{0H}, denoted as R_{0H_1}, quantifies the basic reproduction number for human-to-human transmission. Meanwhile, the second term, R_{0H_2}, accounts for transmission resulting from human interaction with viruses in a contaminated environment. Therefore, (4.1) can be written as

$$R_{0H} = R_{0H_1} + R_{0H_2},$$

where $R_{0H_1} = h_1 + h_2$, $R_{0H_2} = h_3 + h_4$ with

$$h_1 = \frac{\beta_1 S_h^0 \sigma_2}{m_3 m_5}, \quad h_2 = \frac{\beta_1 S_h^0 \theta_2 \sigma_1}{m_3 m_4 m_5}, \quad h_3 = \frac{\beta_3 S_h^0 \rho_h \sigma_2}{m_3 m_5 \mu_C}, \quad \text{and} \quad h_4 = \frac{\beta_3 S_h^0 \rho_h \theta_2 \sigma_1}{m_3 m_4 m_5 \mu_C}.$$

The second equilibrium point is infected animal-free equilibrium point, where $I_r = 0$, meaning there is no disease in the animal population. This equilibrium point can be expressed as

$$E_1 = (S_h^1, V_h^1, E_h^1, Q_h^1, I_h^1, H_h^1, R_h^1, S_r^0, 0, C^1),$$

where

$$S_h^1 = \frac{\Lambda_h m_2}{m_2\hat{\beta} + m_1 m_2 - \epsilon\phi}, \ \hat{\beta} = \frac{\beta_1 I_h^1}{1 + \alpha_1 I_h^1} + \beta_3 C^1, \ V_h^1 = \frac{\epsilon S_h^1}{m_2}, \ E_h^1 = \frac{\hat{\beta} S_h^1}{m_3},$$
$$Q_h^1 = \frac{\sigma_1 E_h^1}{m_4}, \ H_h^1 = \frac{\gamma I_h^1}{m_6}, \ R_h^1 = \frac{\theta_1 Q_h^1 + \nu H_h^1}{\mu_h}, \ C^1 = \frac{\rho_h I_h^1}{\mu_C}, \ I_h^1 = \frac{-b_2 - \sqrt{b_2^2 + 4b_1 b_3}}{-2b_1},$$

with

$$b_1 = m_2 \beta_3 \rho_h \alpha_1,$$
$$b_2 = \alpha_1 \mu_C (m_1 m_2 - \epsilon\phi)(R_{0H_2} - 1) - m_2(\beta_1 \mu_C + \beta_3 \rho_h),$$
$$b_3 = \mu_C (m_1 m_2 - \epsilon\phi)(R_{0H} - 1).$$

Note that $I_h^1 > 0$ if $b_3 > 0$, i.e. $R_{0H} > 1$. So, E_1 exists when $R_{0H} > 1$.

The third equilibrium point is the endemic equilibrium point which indicates that infection is present in all populations. This equilibrium point can be expressed as

$$E_* = (S_h^*, V_h^*, E_h^*, Q_h^*, I_h^*, H_h^*, R_h^*, S_r^*, I_r^*, C^*),$$

where

$$S_h^* = \frac{\Lambda_h m_2}{m_2\beta^* + m_1 m_2 - \epsilon\phi}, \ \beta^* = \frac{\beta_1 I_h^*}{1 + \alpha_1 I_h^*} + \beta_2 I_r^* + \beta_3 C^*, \ V_h^* = \frac{\epsilon S_h^*}{m_2}, \ E_h^* = \frac{\beta^* S_h^*}{m_3}, \ Q_h^* = \frac{\sigma_1 E_h^*}{m_4},$$
$$H_h^* = \frac{\gamma I_h^*}{m_6}, \ R_h^* = \frac{\theta_1 Q_h^* + \nu H_h^*}{\mu_h}, \ S_r^* = \frac{\Lambda_r}{\beta_4 I_r^* + \mu_r}, \ I_r^* = \frac{\mu_r (R_{0R} - 1)}{\beta_4}, \ C^* = \frac{\rho_h I_h^* + \rho_r I_r^*}{\mu_C},$$

and I_h^* is a solution of the following equation.

$$-b_1^* I_h^3 + b_2^* I_h^2 + b_3^* I_h + b_4^* = 0, \tag{4.2}$$

where

$$b_1^* = m_2 m_3 m_4 m_5 \beta_3 \rho_h \alpha_1,$$
$$b_2^* = m_3 m_4 m_5 \left\{\mu_C \alpha_1 (m_1 m_2 - \epsilon\phi)(R_{0H_2} - 1) - m_2 \left[\beta_1 \mu_C + \beta_3 \rho_h + I_r^* \alpha_1 (\beta_2 \mu_C + \beta_3 \rho_r)\right]\right\}$$
$$b_3^* = m_3 m_4 m_5 \mu_C (m_1 m_2 - \epsilon\phi)(R_{0H} - 1) + (\beta_2 \mu_C + \beta_3 \rho_r) m_2 I_r^* \left[\Lambda_h \alpha_1 (m_4 \sigma_2 + \sigma_1 \theta_2) - m_3 m_4 m_5\right],$$
$$b_4^* = \Lambda_h m_2 I_r^* (\beta_2 \mu_C + \beta_3 \rho_r)(m_4 \sigma_2 + \sigma_1 \theta_2).$$

Note that if $R_{0R} > 1$, then $I_r^* > 0$, consequently $b_4^* > 0$. Note also that $b_1^* > 0$, so that, using Descartes' Sign Rule [21], whatever the sign of b_2^* and b_3^*, (4.2) will have at least one positive real root. Thus, model (2.1) has at least one endemic equilibrium point E_* if $R_{0R} > 1$.

5. Stability analysis of E_0 and E_*

To determine the local stability of E_0 and E_*, we linearized the model and obtained the eigenvalues of the Jacobian matrices around the equilibrium point. We then found the Jacobian matrices of the model (2.1) to be as follows.

$$J = \begin{pmatrix} -(\beta+m_1) & \phi & 0 & 0 & -\frac{\beta_1 S_h}{(1+\alpha_1 I_h)^2} & 0 & 0 & 0 & -\beta_2 S_h & -\beta_3 S_h \\ \epsilon & -m_2 & 0 & 0 & 0 & 0 & 0 & 0 & 0 & 0 \\ \beta & 0 & -m_3 & 0 & \frac{\beta_1 S_h}{(1+\alpha_1 I_h)^2} & 0 & 0 & 0 & \beta_2 S_h & \beta_3 S_h \\ 0 & 0 & \sigma_1 & -m_4 & 0 & 0 & 0 & 0 & 0 & 0 \\ 0 & 0 & \sigma_2 & \theta_2 & -m_5 & 0 & 0 & 0 & 0 & 0 \\ 0 & 0 & 0 & 0 & \gamma & -m_6 & 0 & 0 & 0 & 0 \\ 0 & 0 & 0 & \theta_1 & 0 & \nu & -\mu_h & 0 & 0 & 0 \\ 0 & 0 & 0 & 0 & 0 & 0 & 0 & -(\beta_4 I_r + \mu_r) & -\beta_4 S_r & 0 \\ 0 & 0 & 0 & 0 & 0 & 0 & 0 & \beta_4 I_r & \beta_4 S_r - m_7 & 0 \\ 0 & 0 & 0 & 0 & \rho_h & 0 & 0 & 0 & \rho_r & -\mu_C \end{pmatrix}$$

Theorem 5.1. *If $R_0 < 1$, then E_0 is locally asymptotically stable, and unstable if $R_0 > 1$.*

Proof. The characteristic equation of J around E_0 ($J(E_0)$) is obtained as follows (the derivation of (5.1) can be seen in the Appendix).

$$\begin{aligned} &(-\mu_r - \lambda)(-\mu_h - \lambda)(-m_6 - \lambda)[m_7\mu_r(R_{0R} - 1) - \lambda] \\ &[\lambda^2 + (m_1 + m_2)\lambda + m_1 m_2 - \epsilon\phi](\lambda^4 + e_1\lambda^3 + e_2\lambda^2 + e_3\lambda + e_4) = 0, \end{aligned} \tag{5.1}$$

where

$$\begin{aligned} e_1 &= m_3 + m_4 + m_5 + \mu_C, \\ e_2 &= m_3 m_5 (1 - h_1) + m_4\mu_C + (m_4 + \mu_C)(m_3 + m_5), \\ e_3 &= m_3 m_4 m_5 (1 - R_{0H_1}) + m_3 m_5 \mu_C [1 - (h_1 + h_3)] + m_4\mu_C(m_3 + m_5), \\ e_4 &= m_3 m_4 m_5 \mu_C (1 - R_{0H}). \end{aligned}$$

From (5.1) we get $\lambda_1 = -\mu_r < 0$, $\lambda_2 = -\mu_h < 0$, $\lambda_3 = -m_6 < 0$, $\lambda_4 = m_7\mu_r(R_{0R} - 1)$,

$$\lambda^2 + (m_1 + m_2)\lambda + m_1 m_2 - \epsilon\phi = 0, \quad \text{or} \tag{5.2}$$

$$\lambda^4 + e_1\lambda^3 + e_2\lambda^2 + e_3\lambda + e_4 = 0. \tag{5.3}$$

Note that when $R_{0R} < 1$, $\lambda_4 < 0$. Furthermore, because $m_1 + m_2 > 0$ and $m_1 m_2 - \epsilon\phi > 0$, based on the Routh-Hurwitz criterion [19], all roots of (5.2) are negative or have negative real parts. If $R_{0H} < 1$, then $e_1 > 0$, $e_2 > 0$, $e_3 > 0$, and $e_4 > 0$, and it can be shown that $e_1 e_2 e_3 > e_3^2 + e_1^2 e_4$, so by [19], all roots of (5.3) are also negative or have negative real parts. If $R_{0R} > 1$, then $\lambda_4 > 0$, and if $R_{0H} > 1$, then $e_4 < 0$, and by [21], (5.3) will have at least one positive real root. Thus, E_0 is locally asymptotically stable if $R_0 < 1$, and unstable if $R_0 > 1$. □

The local stability of endemic equilibrium E_* is determined using a similar approach to that in Theorem 5.1. Suppose $R_{0R} > 1$ such that there exist an endemic equailibrium E_*. The characteristic

equation of $J(E_*)$ is obtained as follows.

$$(-\mu_h - \lambda)(-m_6 - \lambda)P_1(\lambda)P_2(\lambda) = 0, \tag{5.4}$$

where

$$P_1(\lambda) = \lambda^2 + \frac{\beta_4 \Lambda_r}{m_7}\lambda + m_7\mu_r(R_{0R} - 1),$$
$$P_2(\lambda) = \lambda^6 + q_1\lambda^5 + q_2\lambda^4 + q_3\lambda^3 + q_4\lambda^2 + q_5\lambda + q_6,$$

and

$$\begin{aligned}
q_1 &= m_1 + m_2 + m_3 + m_4 + m_5 + \mu_C,\\
q_2 &= \frac{m_3 m_5 S_h^*}{S_h^0}\left(\varphi - \frac{h_1}{(1+\alpha_1 I_h^*)^2}\right) + (m_1+m_2)(m_3+m_4+m_5+\mu_C)\\
&\quad + m_3(m_4+\mu_C) + m_4(m_5+\mu_C) + m_5\mu_C + \beta^*(m_2+m_3+m_4+m_5+\mu_C) + m_1m_2 - \epsilon\phi,\\
q_3 &= \frac{m_3 m_5 S_h^*}{S_h^0}\left[\mu_C\left(\varphi - \frac{h_1}{(1+\alpha_1 I_h^*)^2} - h_3\right) + m_4\left(\varphi - \frac{R_{0H_1}}{(1+\alpha_1 I_h^*)^2}\right) + (m_1+m_2)\left(\varphi - \frac{h_1}{(1+\alpha_1 I_h^*)^2}\right)\right]\\
&\quad + (\beta^* m_2 + m_1 m_2 - \epsilon\phi)(m_3+m_4+m_5+\mu_C) + m_3\beta^*(m_4+m_5+\mu_C)\\
&\quad + m_3(m_1+m_2)(m_4+\mu_C) + m_4(\beta^*+m_1+m_2)(m_5+\mu_C),\\
q_4 &= \frac{m_3 m_5 S_h^*}{S_h^0}\left[\mu_C(m_1+m_2)\left(\varphi - \frac{h_1}{(1+\alpha_1 I_h^*)^2} - h_3\right) + m_4(m_1+m_2)\left(\varphi - \frac{R_{0H_1}}{(1+\alpha_1 I_h^*)^2}\right)\right.\\
&\quad \left. + (m_1m_2 - \epsilon\phi)\left(\varphi - \frac{h_1}{(1+\alpha_1 I_h^*)^2}\right) + m_4\mu_C\left(\varphi - \frac{R_{0H_1}}{(1+\alpha_1 I_h^*)^2} - R_{0H_2}\right)\right]\\
&\quad + \beta^* m_2\left[m_3(m_4+m_5+\mu_C) + m_4(m_5+\mu_C) + m_5\mu_C\right] + \beta^* m_3 m_4(m_5+\mu_C) + \beta^* m_5\mu_C(m_3+m_4)\\
&\quad + (m_1m_2 - \epsilon\phi)(m_3m_4 + m_4m_5 + m_4\mu_C + m_3\mu_C + m_5\mu_C) + (m_1+m_2)(m_3+m_5)m_4\mu_C,\\
q_5 &= \frac{m_3 m_5 S_h^*}{S_h^0}\left\{(m_1m_2 - \epsilon\phi)\left[m_4\left(\varphi - \frac{R_{0H_1}}{(1+\alpha_1 I_h^*)^2}\right) + \mu_C\left(\varphi - \frac{h_1}{(1+\alpha_1 I_h^*)^2} - h_3\right)\right]\right.\\
&\quad \left. + (m_1+m_2)m_4\mu_C\left(\varphi - \frac{R_{0H_1}}{(1+\alpha_1 I_h^*)^2} - R_{0H_2}\right)\right\} + (m_1m_2 - \epsilon\phi)(m_4+m_5)m_4\mu_C\\
&\quad + \beta^* m_2 m_3 m_4(m_5+\mu_C) + \beta^* m_2 m_5\mu_C(m_3+m_4) + \beta^* m_3 m_4 m_5\mu_C,\\
q_6 &= \frac{(m_1m_2 - \epsilon\phi)m_3m_4m_5\mu_C S_h^*}{S_h^0}\left(\varphi - R_{0H_2} - \frac{R_{0H_1}}{(1+\alpha_1 I_h^*)^2}\right) + \beta^* m_2 m_3 m_4 m_5\mu_C,\\
\varphi &= 1 + \frac{\beta^* m_2}{m_1 m_2 - \epsilon\phi}.
\end{aligned}$$

From (5.4), we get $\lambda_1^* = -\mu_h < 0$ and $\lambda_2^* = -m_6 < 0$. Therefore, the stability of E_* is governed by the roots of $P_1(\lambda)$ and $P_2(\lambda)$. Since all roots of $P_1(\lambda)$ have negative real parts due to the conditions $\beta_4\Lambda_r/m_7 > 0$ and $m_7\mu_r(R_{0R} - 1) > 0$, it remains to establish conditions for $P_2(\lambda)$. According to the Routh-Hurwitz criterion [19], the roots of $P_2(\lambda)$ will have negative real parts if the following conditions hold:

B1. $\frac{R_{0H_1}}{(1+\alpha_1 I_h^*)^2} + R_{0H_2} < \varphi$.
B2. $q_1q_2 - q_3 > 0$.
B3. $q_1q_2q_3 + q_1q_5 - q_1^2q_4 - q_3^2 > 0$.
B4. $q_4(q_1q_2q_3 + q_1q_5 - q_1^2q_4 - q_3^2) + (q_1q_6 - q_2q_5)(q_1q_2 - q_3) + q_5(q_1q_4 - q_5) > 0$.
B5. $(q_4q_5 - q_3q_6)(q_1q_2q_3 + q_1q_5 - q_1^2q_4 - q_3^2) + (2q_1q_5q_6 - q_2q_5^2)(q_1q_2 - q_3) + q_5^2(q_1q_4 - q_5) - q_1^3q_6^2 > 0$.

Condition **B1** ensures all coefficients of $P_2(\lambda)$ are positive. When all these conditions are satisfied, the equilibrium E_* is locally asymptotically stable.

The local stability of E_1 is investigated by proving the existence of forward bifurcation at $R_{0H} = 1$.

6. Forward bifurcation at $R_{0H} = 1$

Forward bifurcation is characterized by the stability transition of the disease-free equilibrium point from stable to unstable as R_0 passes one from below, and the appearance of an asymptotically stable equilibrium point. In this section, we will show the occurrence of forward bifurcation in model (2.1) based on general center manifold theory [6].

Theorem 6.1. *When $R_{0R} < 1$, model (2.1) undergoes forward bifurcation at $R_{0H} = 1$.*

Proof. Suppose β_1 is the bifurcation parameter, then when $R_{0H} = 1$,

$$\beta_1 = \frac{(1 - R_{0H_2})m_3m_4m_5}{S_h^0(m_4\sigma_2 + \theta_2\sigma_1)} = \beta_1^*.$$

Looking again at the characteristic equation of $J(E_0)$ (5.1), when $R_{0H} = 1$, $e_4 = 0$. So, from (5.3), we get

$$\lambda = 0 \quad \text{or} \quad \lambda^3 + e_1\lambda^2 + e_2^*\lambda + e_3^* = 0,$$

where

$$e_2^* = m_3m_5\left(h_1 + R_{0H_2}\right) + m_4\mu_C + (m_4 + \mu_C)(m_3 + m_5) \quad \text{and}$$
$$e_3^* = m_3m_4m_5R_{0H_2} + m_3m_5\mu_C\left(h_1 + h_4\right) + m_4\mu_C(m_3 + m_5).$$

Furthermore, it can be shown that $e_1e_2^* > e_3^*$, so according to [19], the characteristic equation of $J(E_0)$ when $\beta_1 = \beta_1^*$ $(J(E_0), \beta_1^*)$ has one zero root and the other roots are negative or have negative real parts.

Let $W = (w_1 \quad w_2 \quad w_3 \quad w_4 \quad w_5 \quad w_6 \quad w_7 \quad w_8 \quad w_9 \quad w_{10})^T$ be the right eigenvector corresponding to eigenvalue zero of $J(E_0, \beta_1^*)$. By solving the system

$$J(E_0, \beta_1^*)W = \vec{0},$$

it is obtained that

$$w_1 = -\frac{m_2S_h^0(m_4\sigma_2 + \theta_2\sigma_1)(\beta_1^*\mu_C + \beta_3\rho_h)}{m_4m_5\mu_C(m_1m_2 - \epsilon\phi)}, \quad w_2 = -\frac{S_h^0\epsilon(m_4\sigma_2 + \theta_2\sigma_1)(\beta_1^*\mu_C + \beta_3\rho_h)}{m_4m_5\mu_C(m_1m_2 - \epsilon\phi)},$$
$$w_3 = 1, \quad w_4 = \frac{\sigma_1}{m_4}, \quad w_5 = \frac{m_4\sigma_2 + \theta_2\sigma_1}{m_4m_5}, \quad w_6 = \frac{\gamma(m_4\sigma_2 + \theta_2\sigma_1)}{m_4m_5m_6},$$
$$w_7 = \frac{m_5m_6\theta_1\sigma_1 + \nu\gamma(m_4\sigma_2 + \theta_2\sigma_1)}{m_4m_5m_6\mu_h}, \quad w_8 = w_9 = 0, \quad \text{and} \quad w_{10} = \frac{\rho_h(m_4\sigma_2 + \theta_2\sigma_1)}{m_4m_5\mu_C}.$$

Let $V = (v_1 \quad v_2 \quad v_3 \quad v_4 \quad v_5 \quad v_6 \quad v_7 \quad v_8 \quad v_9 \quad v_{10})$ be the left eigenvector corresponding to eigenvalue zero of $J(E_0, \beta_1^*)$. By solving the system

$$VJ(E_0, \beta_1^*) = \vec{0},$$

it is obtained that

$$v_1 = v_2 = v_6 = v_7 = v_8 = 0, \quad v_3 = \frac{m_4\sigma_2 + \theta_2\sigma_1}{m_3\theta_2}, \quad v_4 = 1, \quad v_5 = \frac{m_4}{\theta_2},$$
$$v_9 = -\frac{S_h^0(\beta_2\mu_C + \beta_3\rho_r)(m_4\sigma_2 + \theta_2\sigma_1)}{m_3\theta_2\mu_C(\beta_4y_8^0 - m_7)}, \quad \text{and} \quad v_{10} = \frac{\beta_3S_h^0(m_4\sigma_2 + \theta_2\sigma_1)}{m_3\theta_2\mu_C}.$$

Suppose $\vec{X} = (S_h, V_h, E_h, Q_h, I_h, H_h, R_h, S_r, I_r, C)$ and $\dot{\vec{X}} = \vec{f}$, where f_k is the kth component of $\dot{\vec{X}}$. Note that since $v_1 = v_2 = v_6 = v_7 = v_8 = 0$, multiplying by these components of V will result in zero.

So we get the bifurcation coefficients, a and b, as follows.

$$\begin{aligned}
a &= \sum_{k,i,j=1}^{10} v_k w_i w_j \frac{\partial^2 f_k}{\partial x_i \partial x_j}(E_0, \beta_1^*) \\
&= v_3 w_1 w_5 \frac{\partial^2 f_3}{\partial S_h \partial I_h}(E_0, \beta_1^*) + v_3 w_5 w_1 \frac{\partial^2 f_3}{\partial I_h \partial S_h}(E_0, \beta_1^*) + v_3 w_1 w_{10} \frac{\partial^2 f_3}{\partial S_h \partial C}(E_0, \beta_1^*) \\
&\quad + v_3 w_{10} w_1 \frac{\partial^2 f_3}{\partial C \partial S_h}(E_0, \beta_1^*) \\
&= v_3 w_1 w_5 \beta_1^* + v_3 w_5 w_1 \beta_1^* + v_3 w_1 w_{10} \beta_3 + v_3 w_{10} w_1 \beta_3 \\
&= -\frac{2 m_2 m_3 (m_4 \sigma_2 + \theta_2 \sigma_1)}{S_h^0 \theta_2 (m_1 m_2 - \epsilon \phi)} < 0, \\
b &= \sum_{k,i,j=1}^{10} v_k w_i \frac{\partial^2 f_k}{\partial x_i \partial \beta_1}(E_0, \beta_1^*) = v_3 w_5 \frac{\partial^2 f_3}{\partial I_h \partial \beta_1}(E_0, \beta_1^*) = v_3 w_5 S_h^0 > 0.
\end{aligned}$$

Based on [6], since $a < 0$ and $b > 0$, when $R_{0R} < 1$, model (2.1) undergoes a forward bifurcation at $R_{0H} = 1$. That is, if $R_{0H} < 1$ then E_0 is locally asymptotically stable, and if $R_{0H} > 1$ then E_0 becomes unstable and E_1 is locally asymptotically stable. □

Using the parameter values in Table 1, with $\epsilon = 0.5$, and allowing β_1 to exceed 0.000063, we varied $\beta_1 \in [0, 0.0008]$ such that $R_{0H} \in [0.01, 2.15]$. The resulting forward bifurcation diagram is presented in Fig. 2.

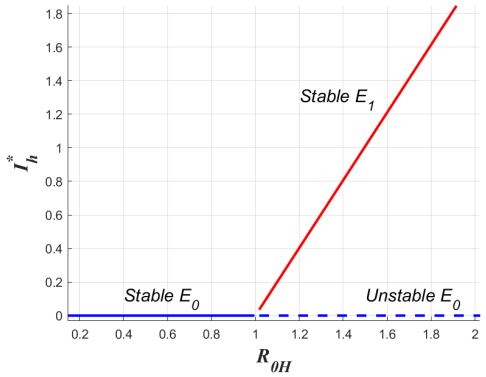

FIGURE 2. Forward bifurcation diagram of model (2.1) at $R_{0H} = 1$ when $R_{0R} < 1$

7. Sensitivity analysis

Sensitivity analysis is performed to evaluate the effect of variations in parameter values on the value of R_0. Note that R_0 of the model (2.1) consists of R_{0H} and R_{0R}, so the sensitivity index can be calculated separately with the following formula [7].

$$\Upsilon_{R_{0H}}^{p} = \frac{p}{R_{0H}} \times \frac{\partial R_{0H}}{\partial p} \quad \text{and} \quad \Upsilon_{R_{0R}}^{q} = \frac{q}{R_{0R}} \times \frac{\partial R_{0R}}{\partial q},$$

where $p \in (\beta_1, \beta_3, \Lambda_h, \epsilon, \phi, \sigma_1, \sigma_2, \theta_1, \theta_2, \mu_h, \mu_c, \gamma, \rho_h, \delta_h)$ and $q \in (\beta_4, \Lambda_r, \mu_r, \delta_r)$ are parameters in R_{0H} and R_{0R}, respectively. Using the parameter values in Table 1 and setting the values of $\epsilon = 0.5$, $\beta_3 = 0.00005$ and $\mu_r = 0.003$, the sensitivity index is presented in Fig. 3. These value of β_3 and μ_r are chosen such that the values of $R_{0H} = 1.97 > 1$ and $R_{0R} = 4.47 > 1$.

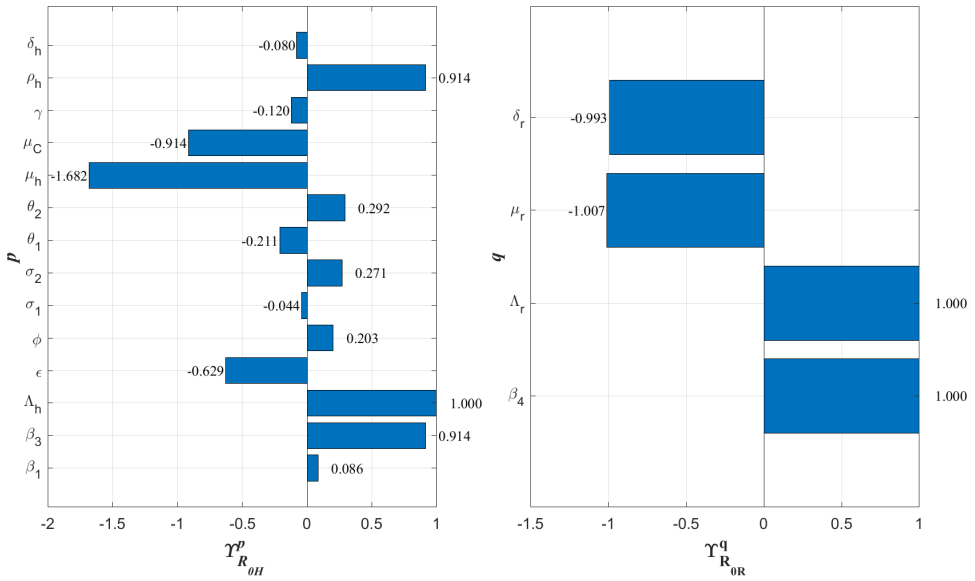

FIGURE 3. The sensitivity index of the parameter in R_{0H} and R_{0R}.

Parameters with a positive sensitivity index indicate that higher values increase R_0, while those with a negative sensitivity index mean that increasing the parameter value reduces R_0. In Fig. 3, there are two parameters with a negative sensitivity index for R_{0R}, namely δ_r and μ_r, and two parameters with a positive sensitivity index, namely Λ_r and β_4. This means that the basic reproduction number for animal-to-animal transmission can be reduced by increasing the mortality rate of animals, δ_r and μ_r, and by decreasing the animal-to-animal transmission rate (β_4) and recruitment rate of susceptible animals (Λ_r).

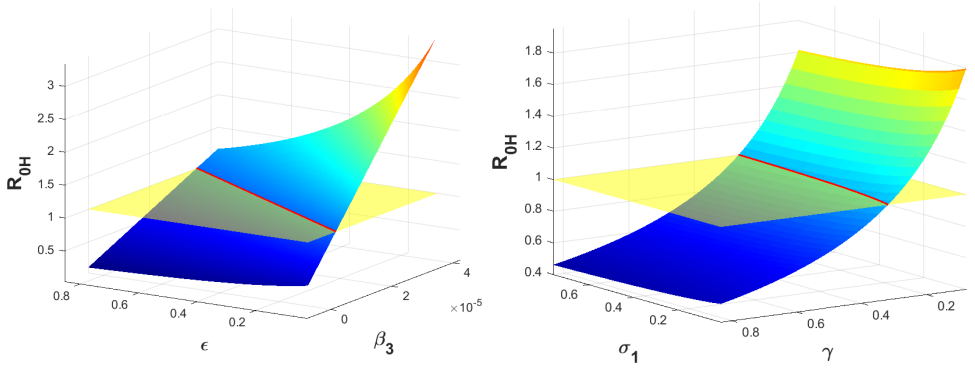

FIGURE 4. 3D plots of R_{0H} of the model (2.1) by varying β_3, ϵ, γ, and σ_1.

For human infections, the interaction between humans and the virus in a contaminated environment (β_3) is one of the most sensitive parameters in R_{0H}, with a strong positive sensitivity index. Reducing β_3 through improved sanitation, decontamination efforts, and public awareness could significantly lower R_{0H}. Conversely, the vaccination rate (ϵ), quarantine rate (σ_1), and treatment rate (γ) have negative sensitivity indices, signifying that increasing these efforts helps push R_{0H} below one, thereby controlling human-to-human transmission. Fig. 4 further supports these findings through a 3D visualization of R_{0H}

with respect to β_3, ϵ, σ_1, and γ. The figure clearly shows that higher values of ϵ, σ_1, and γ contribute to a decrease in R_{0H}, reinforcing the effectiveness of these intervention strategies. Meanwhile, an increase in β_3 results in a rise in R_{0H}, emphasizing the need to mitigate environmental transmission pathways. These sensitivity analysis highlight key intervention points: targeting animal mortality rates, reducing transmission between animals, and implementing effective vaccination, quarantine, and treatment strategies for humans. Controlling the contaminated environment also emerges as a critical measure in minimizing the spread of the disease.

8. Numerical simulations

This section presents numerical simulations using the fourth-order Runge-Kutta method with parameters from Table 1 to verify the analytical results. All initial conditions used in this simulation are selected based on several criteria: they must lie within the feasible region of the model, represent solution orbits from various perspectives in the phase portrait, and be sufficiently close to the equilibrium points to effectively illustrate local stability. The first simulation shows the case where $R_{0R} < 1$ and $R_{0H} < 1$. The phase potrait in Fig. 5 is obtained by setting $\epsilon = 0.5$ and $\alpha_1 = 0.5$. Note that the solution will converge to E_0, meaning that the disease will eventually disappear from the population. This simulation is consistent with Theorem 5.1, that when $R_0 < 1$, E_0 is locally asymptotically stable.

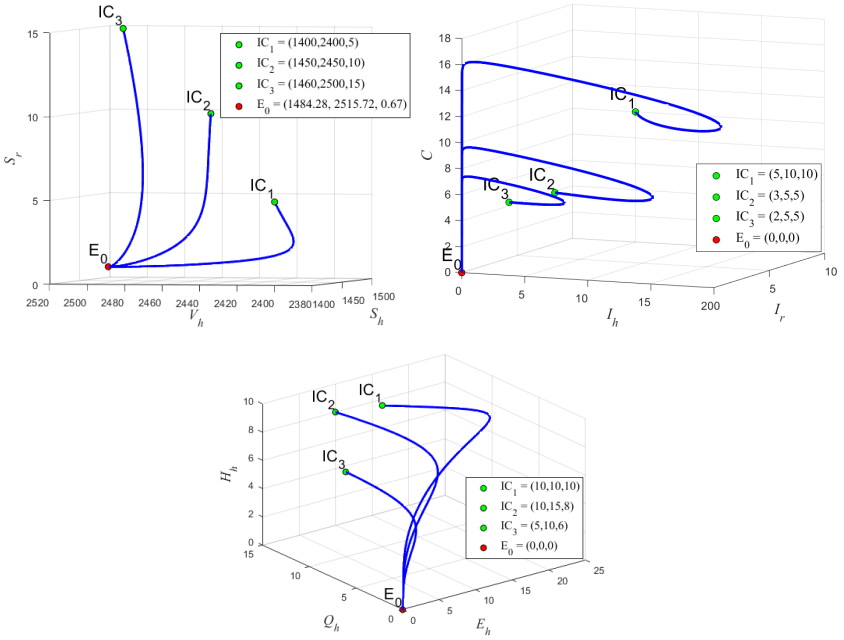

Figure 5. Phase portrait of model (2.1) when $R_{0H} = 0.18$ and $R_{0R} = 0.02$ with several initial conditions (IC), shows that E_0 is locally asymptotically stable.

The second simulation illustrates the effect of ϵ, σ_1, and γ in reducing disease in the human population. Therefore, from previous simulation, we increased β_3 to $\beta_3 = 0.00009$ so that $R_{0H} > 1$. This choice of β_3 is based on sensitivity analysis, which shows that increasing β_3 leads to a higher R_{0H}. We also increased the vaccination rate ϵ (from 0.5 to 0.7) and the quarantine rate σ_1 (from 0.481 to 0.8). This adjustment aims to bring R_{0H} below one, in line with the sensitivity analysis indicating that increasing ϵ, σ_1, and γ can reduce R_{0H}. Next, with the increased values of ϵ and σ_1, the treatment rate γ was varied until $R_{0H} < 1$ was achieved. Using the initial conditions $IC = (1200, 2500, 15, 30, 100, 15, 70, 5, 5, 100)$,

the numerical solution of model (2.1) are obtained and shown in Fig. 6. It can be observed that when $\gamma = 0.03$ or $\gamma = 0.3$ such that $R_{0H} > 1$, the solution converges to E_1. However, when $\gamma = 0.6$, the value of R_{0H} manages to reach less than one, making E_0 locally asymptotically stable. This simulation corresponds to the result in Theorem 6.1 that when $R_{0H} < 1$, E_0 is the only equilibrium point that exists, and it is locally asymptotically stable. Furthermore, this simulation suggests that simultaneously increasing the vaccination rate (ϵ), quarantine of exposed humans (σ_1), and hospitalization of infected humans (γ) can reduce and eventually eliminate the disease from the population.

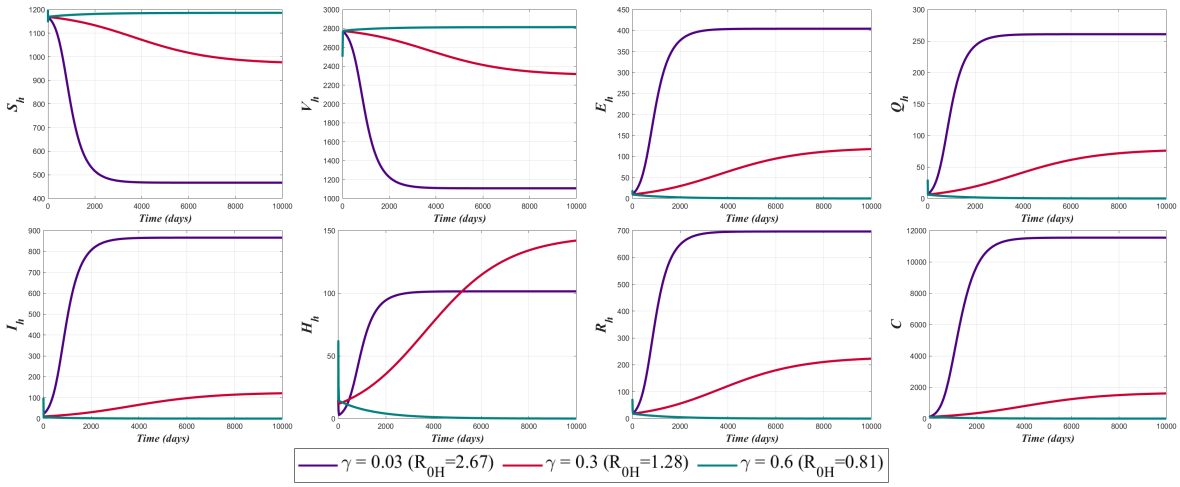

FIGURE 6. The numerical solution of S_h, V_h, E_h, Q_h, I_h, H_h, R_h, and C when $R_{0R} = 0.02$, $\epsilon = 0.7$, and $\sigma_1 = 0.8$, shows that when $R_{0H} > 1$, the solution converges to E_1, while when $R_{0H} < 1$, the solution converges to E_0.

The third simulation is the case where $R_{0R} > 1$. Using the parameter values in Table 1, and setting $\epsilon = 0.5$, $\alpha_1 = 0.5$, and $\mu_r = 0.003$ (from 0.3), we get $R_{0H} = 0.18$ and $R_{0R} = 4.47$. The choice of μ_r is based on the sensitivity analysis that smaller μ_r increasing R_{0R}. The existing equilibrium points are E_0 and E_*, and the Routh-Hurwitz criteria **B1-B5** are satisfied. The phase portrait in Fig. 7 shows E_* is locally asymptotically stable, and E_0 is unstable. This result is consistent with Theorem 5.1 that when $R_0 < 1$, E_0 is unstable. Furthermore, the effect of the saturation constant α_1 is simulated. The value of α_1 is chosen so that the conditions **B1-B5** are satisfied. Therefore, with initial condition $IC = (1480, 2500, 2, 1, 2, 1, 0, 12, 1, 40)$, Fig. 8 shows that the solution converges to E_*. This simulation can be interpreted as the condition when $R_{0R} > 1$, by setting the rate of inhibition in human-to-human transmission (α_1) large enough, it will reduce the number of infected individuals when the disease persists in the population.

9. Conclusions

A compartmental model was developed to describe the behavior of monkeypox spread in human and animal populations and virus persistence in contaminated environments. While previous models have incorporated various factors such as vaccination, quarantine, and hospitalization, they have primarily relied on bilinear or standard incidence rates for human-to-human transmission. Our model advances this work by incorporating a saturated incidence rate, which better reflects the impact of behavioral adaptations as infection levels rise. Additionally, unlike existing models, we integrate both environmental transmission and behavioral-dependent transmission dynamics within a unified framework.

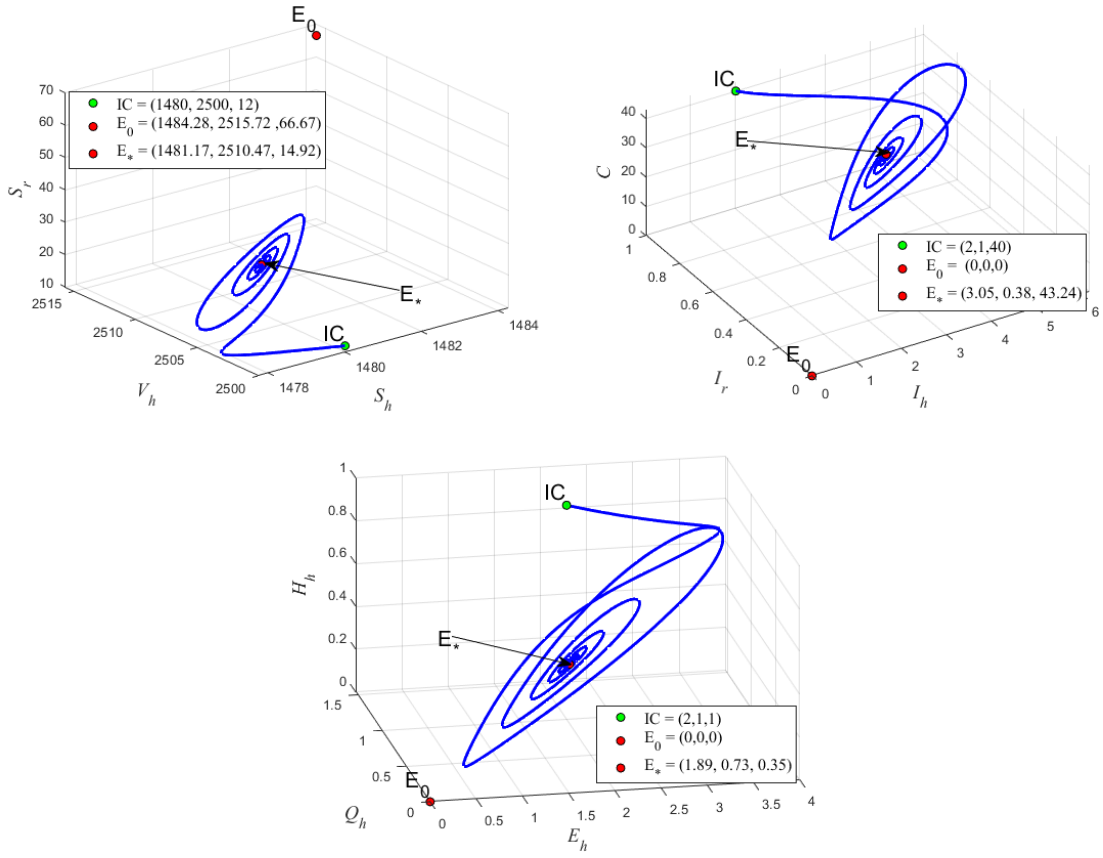

FIGURE 7. Phase portrait of model (2.1) when $R_{0H} = 0.55$, $R_{0R} = 4.14$, and **B1**-**B5** are satisfied, shows that E_* is locally asymptotically stable, while E_0 is unstable.

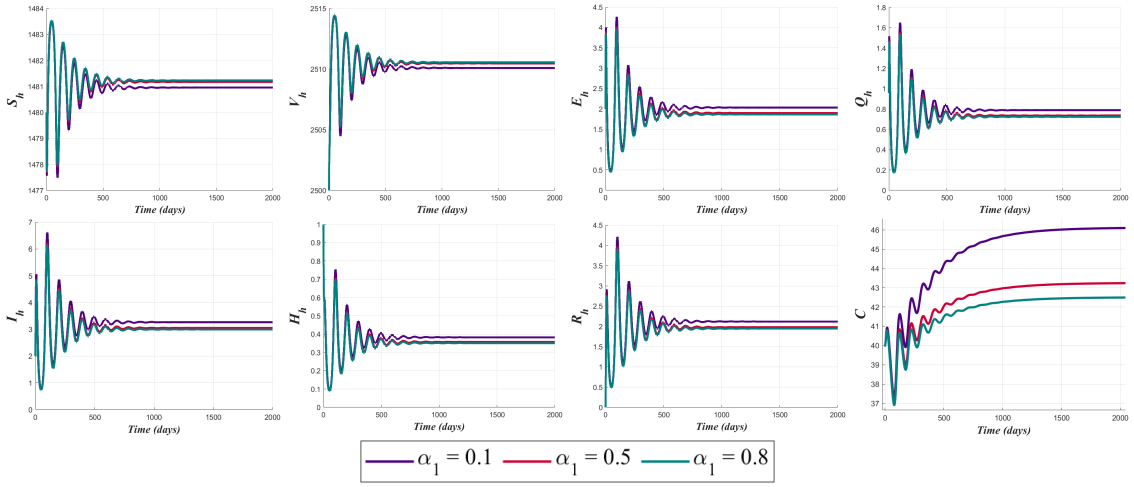

FIGURE 8. The numerical solution of model (2.1) when $R_{0H} = 0.18$, $R_{0R} = 4.47$, and by varying α_1, shows that the solution converges to E_*.

This approach provides a more realistic understanding of monkeypox spread and potential intervention strategies, particularly in outbreak scenarios where individual behaviors play a crucial role in mitigating transmission.

It is identified that the model has three equilibrium points: disease-free, infected animal-free, and endemic. The basic reproduction number of the model consists of the basic reproduction number for virus transmission in human (R_{0H}) and animal (R_{0R}) populations. The local stability criteria of the equilibrium points were obtained, which depend on the basic reproduction number. The analysis also shows that the proposed model exhibits forward bifurcation.

Sensitivity analysis indicates that the effective contact rate between susceptible humans and the virus in a contaminated environment (β_3) is one of the most sensitive parameters in the spread of monkeypox. A smaller β_3 value results in a smaller R_{0H}, eventually reducing it to less than one. As a result, with a particular parameter values such that $R_{0R} < 1$, the disease will disappear in the population. Numerical simulations further suggest that if $R_{0R} < 1$, increasing vaccination on susceptible humans (ϵ), quarantine for exposed humans (σ_1), and hospitalization for infected cases (γ) can eliminate the disease. Conversely, if $R_{0R} > 1$, the disease will persist in the population, and increasing the saturation rate in human-to-human transmission (α_1)—for instance, through public health campaigns promoting hygiene practices to reduce exposure to infected individuals—can help decrease the number of infected individuals and the viruses in the contaminated environment.

Appendix

The characteristic equation of $J(E_0)$ (5.1) is obtained by computing $|J(E_0) - \lambda I| = 0$ where

$$|J(E_0) - \lambda I| = \begin{vmatrix} -m_1-\lambda & \phi & 0 & 0 & -\beta_1 S_h^0 & 0 & 0 & 0 & -\beta_2 S_h^0 & -\beta_3 S_h^0 \\ \epsilon & -m_2-\lambda & 0 & 0 & 0 & 0 & 0 & 0 & 0 & 0 \\ 0 & 0 & -m_3-\lambda & 0 & \beta_1 S_h^0 & 0 & 0 & 0 & \beta_2 S_h^0 & \beta_3 S_h^0 \\ 0 & 0 & \sigma_1 & -m_4-\lambda & 0 & 0 & 0 & 0 & 0 & 0 \\ 0 & 0 & \sigma_2 & \theta_2 & -m_5-\lambda & 0 & 0 & 0 & 0 & 0 \\ 0 & 0 & 0 & 0 & \gamma & -m_6-\lambda & 0 & 0 & 0 & 0 \\ 0 & 0 & 0 & \theta_1 & 0 & \nu & -\mu_h-\lambda & 0 & 0 & 0 \\ 0 & 0 & 0 & 0 & 0 & 0 & 0 & -\mu_r-\lambda & -\beta_4 S_r^0 & 0 \\ 0 & 0 & 0 & 0 & 0 & 0 & 0 & 0 & \beta_4 S_r^0 - m_7 - \lambda & 0 \\ 0 & 0 & 0 & 0 & \rho_h & 0 & 0 & 0 & \rho_r & -\mu_C-\lambda \end{vmatrix}$$

By doing expansion along the eighth column of $|J(E_0) - \lambda I|$, we obtain

$$|J(E_0) - \lambda I| = (-\mu_r - \lambda) \cdot \begin{vmatrix} -m_1-\lambda & \phi & 0 & 0 & -\beta_1 S_h^0 & 0 & 0 & -\beta_2 S_h^0 & -\beta_3 S_h^0 \\ \epsilon & -m_2-\lambda & 0 & 0 & 0 & 0 & 0 & 0 & 0 \\ 0 & 0 & -m_3-\lambda & 0 & \beta_1 S_h^0 & 0 & 0 & \beta_2 S_h^0 & \beta_3 S_h^0 \\ 0 & 0 & \sigma_1 & -m_4-\lambda & 0 & 0 & 0 & 0 & 0 \\ 0 & 0 & \sigma_2 & \theta_2 & -m_5-\lambda & 0 & 0 & 0 & 0 \\ 0 & 0 & 0 & 0 & \gamma & -m_6-\lambda & 0 & 0 & 0 \\ 0 & 0 & 0 & \theta_1 & 0 & \nu & -\mu_h-\lambda & 0 & 0 \\ 0 & 0 & 0 & 0 & 0 & 0 & 0 & \beta_4 S_r^0 - m_7 - \lambda & 0 \\ 0 & 0 & 0 & 0 & \rho_h & 0 & 0 & \rho_r & -\mu_C-\lambda \end{vmatrix}. \quad \text{(A.1)}$$

Next, we expand along the seventh column of (A.1), resulting in

$$|J(E_0)-\lambda I| = (-\mu_r-\lambda)(-\mu_h-\lambda)\cdot \cdot \begin{vmatrix} -m_1-\lambda & \phi & 0 & 0 & -\beta_1 S_h^0 & 0 & -\beta_2 S_h^0 & -\beta_3 S_h^0 \\ \epsilon & -m_2-\lambda & 0 & 0 & 0 & 0 & 0 & 0 \\ 0 & 0 & -m_3-\lambda & 0 & \beta_1 S_h^0 & 0 & \beta_2 S_h^0 & \beta_3 S_h^0 \\ 0 & 0 & \sigma_1 & -m_4-\lambda & 0 & 0 & 0 & 0 \\ 0 & 0 & \sigma_2 & \theta_2 & -m_5-\lambda & 0 & 0 & 0 \\ 0 & 0 & 0 & 0 & \gamma & -m_6-\lambda & 0 & 0 \\ 0 & 0 & 0 & 0 & 0 & 0 & \beta_4 S_r^0 - m_7 - \lambda & 0 \\ 0 & 0 & 0 & 0 & \rho_h & 0 & \rho_r & -\mu_C-\lambda \end{vmatrix}. \tag{A.2}$$

Continuing with an expansion along the sixth column of (A.2) gives

$$|J(E_0)-\lambda I| = (-\mu_r-\lambda)(-\mu_h-\lambda)(-m_6-\lambda)\cdot \cdot \begin{vmatrix} -m_1-\lambda & \phi & 0 & 0 & -\beta_1 S_h^0 & -\beta_2 S_h^0 & -\beta_3 S_h^0 \\ \epsilon & -m_2-\lambda & 0 & 0 & 0 & 0 & 0 \\ 0 & 0 & -m_3-\lambda & 0 & \beta_1 S_h^0 & \beta_2 S_h^0 & \beta_3 S_h^0 \\ 0 & 0 & \sigma_1 & -m_4-\lambda & 0 & 0 & 0 \\ 0 & 0 & \sigma_2 & \theta_2 & -m_5-\lambda & 0 & 0 \\ 0 & 0 & 0 & 0 & 0 & \beta_4 S_r^0 - m_7 - \lambda & 0 \\ 0 & 0 & 0 & 0 & \rho_h & \rho_r & -\mu_C-\lambda \end{vmatrix}. \tag{A.3}$$

Finally, by performing an expansion along the sixth row of (A.3), we get

$$|J(E_0)-\lambda I| = (-\mu_r-\lambda)(-\mu_h-\lambda)(-m_6-\lambda)(\beta_4 S_r^0 - m_7 - \lambda)M, \tag{A.4}$$

where

$$M = \begin{vmatrix} -m_1-\lambda & \phi & 0 & 0 & -\beta_1 S_h^0 & -\beta_3 S_h^0 \\ \epsilon & -m_2-\lambda & 0 & 0 & 0 & 0 \\ 0 & 0 & -m_3-\lambda & 0 & \beta_1 S_h^0 & \beta_3 S_h^0 \\ 0 & 0 & \sigma_1 & -m_4-\lambda & 0 & 0 \\ 0 & 0 & \sigma_2 & \theta_2 & -m_5-\lambda & 0 \\ 0 & 0 & 0 & 0 & \rho_h & -\mu_C-\lambda \end{vmatrix}.$$

After simplification, we get

$$M = [\lambda^2 + (m_1+m_2)\lambda + m_1 m_2 - \epsilon\phi](\lambda^4 + e_1\lambda^3 + e_2\lambda^2 + e_3\lambda + e_4).$$

In (A.4), $\beta_4 S_r^0 - m_7 = m_7\left(\frac{\beta_4 S_r^0}{m_7} - 1\right) = m_7(R_{0R}-1)$.Therefore, the characteristic equation of $J(E_0)$ is obtained as follows.

$$(-\mu_r-\lambda)(-\mu_h-\lambda)(-m_6-\lambda)\,[m_7(R_{0R}-1)-\lambda]$$
$$(\lambda^2 + (m_1+m_2)\lambda + m_1 m_2 - \epsilon\phi)(\lambda^4 + e_1\lambda^3 + e_2\lambda^2 + e_3\lambda + e_4) = 0.$$

References

[1] A. Alshehri and S. Ullah, *Optimal control analysis of Monkeypox disease with the impact of environmental transmission*, AIMS math. **8**(2023), 16926–16960.

[2] E. Alakunle, U. Moens, G. Nchinda, and M. I. Okeke, *Monkeypox virus in Nigeria: Infection biology, epidemiology, and evolution*, Viruses, **12**(2020): 1257.

[3] M. Badole, R. Bhardwaj, R. Joshi, and P. Konar, *Stability analysis of a SIQR epidemic compartmental model with saturated incidence rate, vaccination and elimination strategies*, Results Control Optim. **16**(2024): 100459.

[4] C. Bhunu and S. Mushayabasa, *Modelling the transmission dynamics of pox-like infections*, IAENG Int. J. Appl. Math. **41**(2011), 141–149.

[5] V. Capasso and G. Serio, *A generalization of the Kermack-McKendrick deterministic epidemic model*, Math. Biosci. **42**(1978), 43–61.

[6] C. Castillo-Chavez and B. Song, *Dynamical models of tuberculosis and their applications*, Math. Biosci. Eng. **1**(2004), 361–404.
[7] N. Chitnis, J. M. Hyman, and J. M. Cushing, *Determining important parameters in the spread of malaria through the sensitivity analysis of a mathematical model*, Bull Math Biol. **70**(2008), 1272-1296.
[8] S. A. Guagliardo et al., *Monkeypox virus infections after 2 preexposure doses of JYNNEOS vaccine—United States, May 2022–May 2024*, MMWR Morb. Mortal. Wkly. Rep. **73**(2024), 460–466.
[9] Y. Jahan, *Monkeypox is an emerging threat to low-middle-income countries amid COVID-19*, Ann. med. surg. **80**(2022): 104344.
[10] W. N. Li and W. Sheng, *Some Gronwall Type Inequalities on Time Scales*, J. Math. Inequal. **4**(2010), 67-76.
[11] C. E. Madubueze, I. O. Onwubuya, G. N. Nkem, and Z. Chazuka, *The transmission dynamics of the monkeypox virus in the presence of environmental transmission*, Front. Appl. Math. Stat. **8**(2022): 1061546.
[12] S. Majee, S. Jana, and T. K. Kar, *Dynamical analysis of monkeypox transmission incorporating optimal vaccination and treatment with cost-effectiveness*, Chaos. **33**(2023): 043103.
[13] *Mpox*, https://ourworldindata.org/mpox, accessed August 24, 2024.
[14] M. Martcheva, *Introduction to Mathematical Epidemiology*, Springer, New York, 2015.
[15] J. D. Murray, *Mathematical Biology I. An Introduction*, Springer, New York, 2011.
[16] W. Okongo, J. O. Abonyo, D. Kioi, S. E. Moore, and S. N. Aguegboh, *Mathematical modeling and optimal control analysis of monkeypox virus in contaminated environment*, Model. Earth Syst. Environ. **10**(2024), 3969–3994.
[17] O. J. Peter et al., *Transmission dynamics of monkeypox virus: A mathematical modeling approach*, Model. Earth Syst. Environ. **8**(2021), 3423–3434.
[18] P. Saha and U. Ghosh, *Complex dynamics and control analysis of an epidemic model with non-monotone incidence and saturated treatment*, Int. J. Dyn. Contr. **11**(2023), 301-323.
[19] D. A. Sanchez, R. C. Allen, and W. T. Kyner, *Differential Equations. 2nd Edition*, Addison-Wesley Pub. Co, Reading, 1988.
[20] S. Usman and I. Isa Adamu, *Modeling the transmission dynamics of the monkeypox virus infection with treatment and vaccination interventions*, Journal of Applied Mathematics and Physics, **5**(2017), 2335–2353.
[21] S. Wiggins, *Introduction to Applied Nonlinear Dynamical Systems and Chaos*, Springer International Publishing, New York, 2003.
[22] J. Zhang, J. Jia, and X. Song, *Analysis of an SEIR epidemic model with saturated incidence and saturated treatment function*, ScientificWorldJournal, **2014**(2014): 910421.

B. V. J. Possumah, corresponding author, Department of Mathematics, Faculty of Mathematics and Natural Sciences, University of Brawijaya, Malang 65145, Indonesia
Email address: brazilvargas@student.ub.ac.id

W. M. Kusumawinahyu, Department of Mathematics, Faculty of Mathematics and Natural Sciences, University of Brawijaya, Malang 65145, Indonesia
Email address: wmuharini@ub.ac.id

Trisilowati, Department of Mathematics, Faculty of Mathematics and Natural Sciences, University of Brawijaya, Malang 65145, Indonesia
Email address: trisilowati@ub.ac.id